

Potential GlueX Physics During the First Two Years of 12 GeV Running

GlueX-doc-621

Curtis A. Meyer
Carnegie Mellon University

20 April, 2006

Abstract

This note evaluates what the expected event rates will be in the GlueX detector during its first two years of running. The distribution of these events into bins for physics analysis is discussed. These are then coupled with known cross sections and interesting physics to identify a potential physics that can be carried out during the first two years of running with GlueX. Such a program includes calibration studies, non-hybrid physics and a solid initial mapping of the exotic hybrid nonets.

1 Introduction

This document identifies the physics that should be possible in GlueX during the first two years of running at 12 GeV. During this period, assumptions will be made about the beam rate. The material in this note is based on two earlier GlueX notes [2] and [3].

2 Hybrid Mesons

Models that predict hybrid mesons predict eight nonets of these states. The spin, parity and C-parity of of these as well as the particle names are shown in Table 1. In the sense that hybrid mesons are just excitations of the gluon field binding the quarks, hybrids should be produced in all reactions which populate the excited $q\bar{q}$ spectrum. However, it is believed that the spin of the initial particle will likely be transferred directly into the spin of the $q\bar{q}$ system in the hybrid. This means that beams of π 's and K 's are likely to produce hybrids built on spin zero, ($S = 0$), objects, 1^{--} and 1^{++} . Similarly, beams of spin one particles are more likely to produce hybrids built on spin-aligned quarks, ($S = 1$), 0^{+-} , 0^{-+} , 1^{+-} , 1^{-+} , 2^{+-} and 2^{-+} . Modulo effects of these assumptions, hybrids should be produced as strongly as other states.

J^{PC}	$S_{q\bar{q}}$	Particle Name			
		$u\bar{d}, d\bar{u}$	$u\bar{u} + d\bar{d}$	$s\bar{s}$	
1^{++}	$S = 0$	a_1	f_1	f_1'	non-exotic
1^{--}	$S = 0$	ρ_1	ω_1	ϕ_1	non-exotic
0^{-+}	$S = 1$	π_0	η_0	η_0'	non-exotic
0^{+-}	$S = 1$	b_0	h_1	h_1'	<i>exotic</i>
1^{-+}	$S = 1$	π_1	η_1	η_1'	<i>exotic</i>
1^{+-}	$S = 1$	b_1	h_1	h_1'	non-exotic
2^{-+}	$S = 1$	π_2	η_2	η_2'	non-exotic
2^{+-}	$S = 1$	b_2	h_2	h_2'	<i>exotic</i>

Table 1: A list of the particles in the eight nonets of predicted hybrid mesons. The six nonets with quark and antiquark in an $S = 1$ state are the most likely to be produced in photo production. Of these $S = 1$ states, half have exotic quantum numbers. Not shown in this table are the strangeness 1 kaonic states.

Independent of what is produced, three of the eight nonets have J^{PC} quantum numbers that cannot be built out of simple quark-antiquark systems. These are known as exotic quantum number states, or simply *exotics*. It is these exotic nonets, 0^{+-} , 1^{-+} and 2^{+-} that will be of particular interest to GlueX in the first years of running. Being able to establish one or more of these nonets is the primary goal of the experiment. In order to do this, observations of more than one state in a given nonet need to be made. In addition, identifying more than just one nonet is important.

2.1 Masses of Hybrid Mesons

Lattice QCD calculations provide our most accurate estimate to the masses of hybrid mesons. While these calculations have progressively gotten better, they are still limited by a number of systematic effects. The most significant of these is that all calculations to date have been performed in the *quenched approximation*. In addition to this, the calculations are made with varying quark masses, and then extrapolated to the light-quark limit. In fact, all efforts to date calculate what is effectively the $s\bar{s}$ member of the nonet, and then some approximation is made to move estimate the $u\bar{u}/d\bar{d}$ mass. The bottom line is that no one would be surprised if the true hybrid masses differed by $0.2 \text{ GeV}/c^2$ from the best predictions.

2.1.1 The π_1 Mass

One of the earliest predictions for hybrids comes from the flux-tube model in which all eight hybrid nonets are degenerate with a mass of about $1.9 \text{ GeV}/c^2$. Lattice QCD calculations consistently show that the exotic 1^{-+} nonet is the lightest. Table 2 lists predictions made over the last several years for the mass of the π_1 and η_1 . These results fall in the range of 1.8 to $2.1 \text{ GeV}/c^2$, with an average about in the middle of these numbers. When it is available in the publication, we report the mass of the $s\bar{s}$ state in addition to the light-quark state.

2.1.2 Mass Splittings of Exotic Nonets

There are fewer predictions for the masses of the other exotic-quantum number states. Bernard [5] calculate the splitting between the 0^{+-} and the 1^{-+} state to be about $0.2 \text{ GeV}/c^2$ with large errors. They later calculate this

Collab.	Author		1^{-+} Mass (GeV/c^2)	
	Year	Ref.	$u\bar{u}/d\bar{d}$	$s\bar{s}$
UKQCD	(1997)	[4]	1.87 ± 0.20	2.0 ± 0.2
MILC	(1997)	[5]	$1.97 \pm 0.09 \pm 0.30$	$2.170 \pm 0.080 \pm 0.30$
MILC	(1999)	[6]	$2.11 \pm 0.10 \pm (sys)$	
SESAM	(1998)	[7]	1.9 ± 0.20	
Mei& Luo	(2003)	[8]	$2.013 \pm 0.026 \pm 0.071$	
Bernard <i>et al.</i>	(2004)	[9]	1.792 ± 0.139	2.100 ± 0.120

Table 2: Recent results for the light-quark 1^{-+} hybrid meson masses. For the charmonium spectrum, the difference is taken from the $1S$ state. The table is based on a similar table in [10].

with a clover action [6] and find a splitting of 0.270 ± 0.2 . The SESAM collaboration [7] has one such calculation, the results of which are shown in Table 3.

Multiplet	J^{PC}	Mass
π_1	1^{-+}	$1.9 \pm 0.2 \text{ GeV}/c^2$
b_2	2^{+-}	$2.0 \pm 0.11 \text{ GeV}/c^2$
b_0	0^{+-}	$2.3 \pm 0.6 \text{ GeV}/c^2$

Table 3: Estimates of the masses of exotic quantum number hybrids.

While the exact masses of hybrids are still an open question, the best predictions point to a numbers in the 1.8 to $2.5 \text{ GeV}/c^2$ mass range. This is the range over which the GlueX experiment has been optimized to search.

2.2 Hybrid Decays

The simplest predictions for hybrid decays are to simply determine what decays are allowed by basic conservation in strong decays: isospin, parity, C-parity and G-parity. Such simple calculations leads to a list of allowed hybrid decays that can guide searches for these states.

As an example of this, consider the b_2 hybrid: $(I^G)J^{PC} = (1^+)2^{+-}$ and consider its decay into a pseudo-scalar, (0^{-+}) and a vector meson, (1^{--}) . We can add the J^{PC} of these two mesons together and include an additional angular momentum, L , between the two mesons. Doing this yields the following

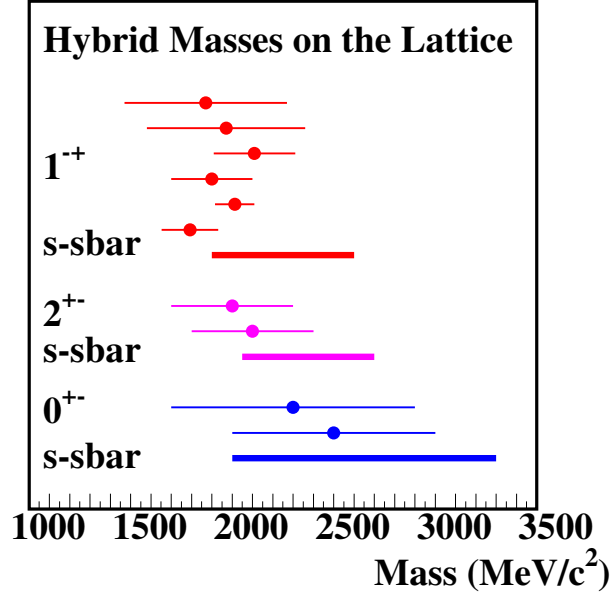


Figure 1: A graphical summary of the mass calculations for hybrids.

lists of allowed quantum numbers for decays with L up to 2.

$$\begin{aligned}
 0^{-+} + 1^{--} \quad L = 0 \quad & 1^{+-} \\
 0^{-+} + 1^{--} \quad L = 1 \quad & 0^{--}, 1^{--}, 2^{--} \\
 0^{-+} + 1^{--} \quad L = 2 \quad & 1^{+-}, \underline{2^{+-}}, 3^{+-}
 \end{aligned}$$

The one exotic J^{PC} that can be reached is 2^{+-} which occurs when we have $L = 2$ between the two mesons. We next consider G -parity which is positive for the b_2 . In order to get a positive G -parity, either both daughter mesons must have positive G -parity or both must have negative G -parity. The meson combinations that allow for this are listed as follows.

$$\begin{aligned}
 \pi\omega \quad I = 1 \quad G = +1 \\
 \pi\phi \quad I = 1 \quad G = +1 \\
 \eta\rho \quad I = 1 \quad G = +1
 \end{aligned}$$

$$\eta'\rho \quad I = 1 \quad G = +1$$

From this, we conclude that there are four possible pseudo-scalar plus vector decays of the b_2 hybrid. As a note, it is now trivial to do the h_2 as well. This is isospin zero with negative G-parity, so the two daughters must have opposite G-parity, but the same isospin. This leads to the five decays given below.

$$\begin{aligned} \pi\rho & \quad I = 0 \quad G = -1 \\ \eta\omega & \quad I = 0 \quad G = -1 \\ \eta\phi & \quad I = 0 \quad G = -1 \\ \eta'\omega & \quad I = 0 \quad G = -1 \\ \eta'\phi & \quad I = 0 \quad G = -1 \end{aligned}$$

Such arguments allow us to build up the entries in the following Tables which show many possible decays for the various hybrid mesons. In order to minimize repetition, we note that the two $I = 0$ states, $u\bar{u}$ and $s\bar{s}$, both have the same set of allowed decays. However, the OZI-rule will suppress or enhance certain modes. The decays of the b_0 are given in Table 4 and the decays of the h_0 is in Table 5. The spin one states are the π_1 , in Table 6, and the η_1 in Table 7. Finally, the spin two states are the b_2 , see Table 8 and the h_2 shown in Table 9. We should emphasize that these are not exhaustive lists of decays. In particular, the decays involving open strangeness, (kaons), are not listed here. There may also be other states if the mass of a particular hybrid is large enough. We should also not that just because a particular decay is allowed does not mean that it will happen. There may well be other physics reasons which suppress some decays, or significantly enhance others.

State	L	Decays			
b_0	$L = 1$	πh_1	$\pi h_1'$	ηb_1	$\eta' b_1$
b_0	$L = 1$	ρf_0	$\rho f_0'$	ωa_0	ϕa_0
b_0	$L = 1$	ρf_1	$\rho f_1'$	ωa_1	ϕa_1
b_0	$L = 1$	$\pi\pi(1300)$			

Table 4: Decays of the $(I^G)J^{PC} = (1^+)0^{+-}$ b_0 hybrid meson.

Predictions for the widths of hybrids are currently based on model calculations with the most recent work [11] given in Table 10 for states with exotic

State	L	Decays				
h_0	$L = 1$	πb_1	ηh_1	$\eta h_1'$	$\eta' h_1$	$\eta' h_1'$
h_0	$L = 1$	ρa_0	ωf_0	$\omega f_0'$	ϕf_0	$\phi f_0'$
h_0	$L = 1$	ρa_1	ωf_1	$\omega f_1'$	ϕf_1	$\phi f_1'$
h_0	$L = 1$	$\eta \eta'$	$\eta \eta(1295)$	$\eta \eta(1440)$		
h_0	$L = 1$	$\eta' \eta(1295)$	$\eta' \eta(1440)$	$\eta(1295) \eta(1440)$		

Table 5: Decays of the $(I^G)J^{PC} = (1^+)0^{+-}$ h_0 and h_0' hybrid mesons.

State	L	Decays			
π_1	$L = 0$	$\pi^\pm b_1$	πb_1^\pm		
π_1	$L = 1$	$\pi^\pm \rho$	$\pi \rho^\pm$		
π_1	$L = 0$	πf_1	$\pi f_1'$	ηa_1	$\eta' a_1$
π_1	$L = 1$	$\pi \eta(1295)$	$\pi \eta(1440)$	$\eta \pi(1300)$	$\eta' \pi(1300)$
π_1	$L = 2$	πf_2	$\pi f_2'$	ηa_2	$\eta' a_2$

Table 6: Decays of the $(I^G)J^{PC} = (1^-)1^{-+}$ π_1 hybrid meson.

State	L	Decays				
η_1	$L = 1$	$\omega \phi$				
η_1	$L = 0$	πa_1	ηf_1	$\eta f_1'$	$\eta' f_1$	$\eta' f_1'$
η_1	$L = 1$	$\pi \pi(1300)$	$\eta \eta(1295)$	$\eta \eta(1440)$	$\eta' \eta(1295)$	$\eta' \eta(1440)$
η_1	$L = 2$	πa_2	ηf_2	$\eta f_2'$	$\eta' f_2$	$\eta' f_2'$

Table 7: Decays of the $(I^G)J^{PC} = (0^+)1^{-+}$ η_1 and η_1' hybrid mesons.

State	L	Decays			
b_2	$L = 2$	$\pi \omega$	$\pi \phi$	$\eta \rho$	$\eta' \rho$
b_2	$L = 1$	ωa_0	ϕa_0	ρf_0	$\rho f_0'$
b_2	$L = 1$	ωa_1	ϕa_1	ρf_1	$\rho f_1'$
b_2	$L = 1$	ωa_2	ϕa_2	ρf_2	$\rho f_2'$
b_2^\pm	$L = 1$	ηb_1^\pm	$\eta' b_1^\pm$	$h_1 \pi^\pm$	$h_1' \pi^\pm$
b_2^\pm	$L = 1$	$\pi^\pm a_2$	πa_2^\pm		

Table 8: Decays of the $(I^G)J^{PC} = (1^+)2^{+-}$ b_2 hybrid meson.

quantum numbers, and in Table 11 for hybrids with normal $q\bar{q}$ quantum numbers. As can be seen, a number of these states are expected to be broad. In particular, most of the 0^{+-} exotic nonet are quite broad. However, states in

State	L	Decays				
h_2	$L = 2$	$\pi\rho$	$\eta\omega$	$\eta\phi$	$\eta'\omega$	$\eta'\phi$
h_2	$L = 1$	ρa_0	ωf_0	$\omega f_0'$	ϕf_0	$\phi f_0'$
h_2	$L = 1$	ρa_1	ωf_1	$\omega f_1'$	ϕf_1	$\phi f_1'$
h_2	$L = 1$	ρa_2	ωf_2	$\omega f_2'$	ϕf_2	$\phi f_2'$
h_2	$L = 1$	πb_1	ηh_1	$\eta h_1'$	$\eta' h_1$	$\eta' h_1'$

Table 9: Decays of the $(I^G)J^{PC} = (0^-)2^{+-}$ h_2 and h_2' hybrid mesons.

both the 2^{+-} and the 1^{-+} nonets have much narrower expected widths. The normal quantum numbers states will be more difficult to disentangle as they are likely to mix with nearby normal $q\bar{q}$ states. Finally, the expected decay modes of these states involve daughters that in turn decay. This makes the overall reconstruction more complicated than simple pseudo-scalar mesons.

However, these decays can be used as a guideline when looking for these states. Almost all models of hybrid mesons predict that the ground state ones will not decay to identical pairs of mesons, and that the decays to an $(L = 0)(L = 1)$ pair is the favored decay mode. Essentially, the one unit of angular momentum in the flux-tube has to go into internal orbital angular momentum of a $q\bar{q}$ pair. In addition, the nonet with non $q\bar{q}$ quantum numbers provide a striking signal for these objects. It is also true that lattice calculations predict that the 1^{-+} nonet, (exotic) is the lightest (see table 2). Above this, the exotic 0^{+-} and the 2^{+-} are the next lightest. It is also important to keep in mind that the splittings between nonets is due to the gluonic degrees of freedom, so a measurement of this quantity can provide insight into the confining potential of QCD.

3 Known and Estimated Photo-production Cross Sections

While the total hadronic cross section is interesting in determine the abilities of the detector and the data acquisition system, the physics is actually obtained from individual channels. There are some data on specific cross sections, and Table 12 shows the measured cross sections for various final states using roughly 9 GeV photons. Most of these cross sections are based on at most a few thousand events, as such we can anticipate large errors in

Particle	$\mathbf{J}^{\mathbf{PC}}$	Total Width MeV		Large Decays
		[11]	[12]	
π_1	1^{-+}	81 – 168	117	$b_1\pi, \rho\pi, \eta(1295)\pi$
η_1	1^{-+}	59 – 158	107	$a_1\pi, \pi(1300)\pi$
η'_1	1^{-+}	95 – 216	172	$K_1(1400)K, K_1(1270)K, K^*K$
b_0	0^{+-}	247 – 429	665	$\pi(1300)\pi, h_1\pi$
h_0	0^{+-}	59 – 262	94	$b_1\pi$
h'_0	0^{+-}	259 – 490	426	$K(1460)K, K_1(1270)K$
b_2	2^{+-}	5 – 11	248	$a_2\pi, a_1\pi, h_1\pi$
h_2	2^{+-}	4 – 12	166	$b_1\pi, \rho\pi$
h'_2	2^{+-}	5 – 18	79	$K_1(1400)K, K_1(1270)K, K_2^*(1430)K$

Table 10: Exotic quantum number hybrid width and decay predictions.

Particle	$\mathbf{J}^{\mathbf{PC}}$	Total Width MeV		Large Decays
		[11]	[12]	
ρ	1^{--}	70 – 121	112	$a_1\pi, \omega\pi, \rho\pi$
ω	1^{--}	61 – 134	60	$\rho\pi, \omega\eta, \rho(1450)\pi$
ϕ	1^{--}	95 – 155	120	$K_1(1400)K, K^*K, \phi\eta$
a_1	1^{++}	108 – 204	269	$\rho(1450)\pi, \rho\pi, K^*K$
h_1	1^{++}	43 – 130	436	$K^*K, a_1\pi$
h'_1	1^{++}	119 – 164	219	$K^*(1410)K, K^*K$
π	0^{-+}	102 – 224	132	$\rho\pi, f_0(1370)\pi$
η	0^{-+}	81 – 210	196	$a_0(1450)\pi, K^*K$
η'	0^{-+}	215 – 390	335	$K_0^*K, f_0(1370)\eta, K^*K$
b_1	1^{+-}	177 – 338	384	$\omega(1420)\pi, K^*K$
h_1	1^{+-}	305 – 529	632	$\rho(1450)\pi, \rho\pi, K^*K$
h'_1	1^{+-}	301 – 373	443	$K^*(1410)K, \phi\eta, K^*K$
π_2	2^{-+}	27 – 63	59	$\rho\pi, f_2\pi$
η_2	2^{-+}	27 – 58	69	$a_2\pi$
η'_2	2^{-+}	38 – 91	69	K_2^*K, K^*K

Table 11: Non-exotic quantum number hybrid width and decay predictions.

many of them. However, the bottom line is that many of these cross sections are on the order of $1\mu b$.

Using the known cross sections in Table 12, we would like to try an estimate what the cross sections are for some more specific final states. Clearly

Reaction	σ
$\gamma p \rightarrow p\pi^+\pi^- X^{neut}$	$20\mu b$
$\gamma p \rightarrow p\pi^+\pi^-\pi^0$	$10\mu b$
$\gamma p \rightarrow n\pi^+\pi^+\pi^- X^{neut}$	$20\mu b$
$\gamma p \rightarrow pK^+K^- X^{neut}$	$1\mu b$
$\gamma p \rightarrow f_2(1270)p$	$1\mu b$
$\gamma p \rightarrow a_2^+(1320)n$	$1\mu b$
$\gamma p \rightarrow b_1^0(1235)p$	$1\mu b$
$\gamma p \rightarrow \rho'(1465)p$	$1\mu b$
$\gamma p \rightarrow \rho(770)p$	$20\mu b$
$\gamma p \rightarrow \omega p$	$2\mu b$
$\gamma p \rightarrow \phi p$	$0.4\mu b$

Table 12: A compilation of known cross sections for photo production at about 9 GeV photon energy.

the accuracy of the accuracy of these estimates are not great, but factors of a few errors are probably no unreasonable. As such, we have quote most of these estimates as ranges rather than an absolute number. In Table 13 we show estimates to various final states. As a note, some of these are estimates based on CLAS numbers from 2 to 4 GeV photon energies. For example, the $\eta\pi^+\pi^-$ is between 5 and 10% of the $\pi^+\pi^-\pi^0$ channel.

4 Event Rate Calculations

In order to make basic event rate calculations, it is necessary to make several assumptions about the running conditions during the first one to two years of running at 12 GeV. During the initial start up of both the accelerator and the detector, it is reasonable to assume that not all parameters will be finalized and the rates quoted in the Design Report [1] may only be met towards the end of this period. Before starting, we will carry out a simple rate calculation to confirm that we are consistent with rates quoted in the GlueX Design Report.

The total event rate is given by the expression in equation 1. The event rate is N_{evt} , the total cross section is σ_t , the number of scattering centers per unit area is N_t and the photon beam rate is N_γ .

$$N_{evt} = \sigma_t \cdot N_t \cdot N_\gamma \quad (1)$$

$\gamma p \rightarrow p\pi^+\pi^-\pi^0$	5–10 μb
$\gamma p \rightarrow n\pi^+\pi^+\pi^-$	5–10 μb
$\gamma p \rightarrow p\pi^+\pi^0\pi^0$	5–10 μb
$\gamma p \rightarrow p\pi^+\pi^-\pi^+\pi^-$	1 – 3 μb
$\gamma p \rightarrow p\pi^+\pi^-\pi^0\pi^0$	1 – 3 μb
$\gamma p \rightarrow p\pi^0\pi^0\pi^0\pi^0$	1 – 3 μb
$\gamma p \rightarrow n\pi^+\pi^-\pi^+\pi^0$	1 – 3 μb
$\gamma p \rightarrow n\pi^+\pi^0\pi^0\pi^0$	1 – 3 μb
$\gamma p \rightarrow p\pi^+\pi^-\pi^+\pi^-\pi^0$	1 – 3 μb
$\gamma p \rightarrow p\pi^+\pi^-\pi^0\pi^0\pi^0$	1 – 3 μb
$\gamma p \rightarrow p\pi^0\pi^0\pi^0\pi^0\pi^0$	1 – 3 μb
$\gamma p \rightarrow n\pi^+\pi^-\pi^+\pi^-\pi^+$	1 – 3 μb
$\gamma p \rightarrow n\pi^+\pi^-\pi^+\pi^0\pi^0$	1 – 3 μb
$\gamma p \rightarrow n\pi^+\pi^0\pi^0\pi^0\pi^0$	1 – 3 μb
$\gamma p \rightarrow p\pi^0\omega$	1 μb
$\gamma p \rightarrow n\pi^+\omega$	1 μb
$\gamma p \rightarrow p\pi^+\pi^-\omega$	0.1–0.5 μb
$\gamma p \rightarrow p\pi^0\pi^0\omega$	0.1–0.5 μb
$\gamma p \rightarrow n\pi^+\pi^0\omega$	0.1–0.5 μb
$\gamma p \rightarrow p\pi^+\pi^-\eta$	0.2–1.0 μb
$\gamma p \rightarrow p\pi^0\pi^0\eta$	0.2–1.0 μb
$\gamma p \rightarrow p\eta\eta$	0.05–0.2 μb
$\gamma p \rightarrow p\omega\eta$	0.05–0.2 μb
$\gamma p \rightarrow p\omega\omega$	0.05–0.2 μb
$\gamma p \rightarrow p\eta\eta'$	0.05–0.2 μb

Table 13: Estimated cross sections for various final states of interest in searching for hybrid mesons.

The total hadronic cross-section, σ_t , for the reaction:

$$\gamma p \rightarrow \text{Anything}$$

at a photon energy of $E_\gamma = 9 \text{ GeV}$ is known to be about

$$\sigma_t = 120 \mu b.$$

The GlueX target is a 30 cm long column of liquid Hydrogen. Using this length and known properties of liquid Hydrogen, we calculate that the number of scattering centers per unit area is given as:

$$\begin{aligned} N_t &= 12.6 \times 10^{23} \text{ cm}^{-2} \text{ or} \\ N_t &= 1.26 b^{-1}. \end{aligned}$$

Finally, we take that the ultimate beam rate in GlueX is

$$N_{\text{gamma}} = 1 \times 10^8 \gamma/s.$$

Putting all this information into equation 1, we find that the event rate in GlueX can be written as:

$$N_{\text{evt}} = (120 \mu b) \times (1.26 b^{-1}) \times (10^8 s^{-1}).$$

Multiplying the numbers out, we arrive at a rate of

$$N_{\text{evt}} \sim 15 \text{ kHz}.$$

This number is in very good agreement with the total hadronic event rate given in the GlueX design report [1].

5 Estimated Data Yields and Distributions

5.1 Estimated Data Rates

Using typical cross sections from the previous section, we can now estimate how many events could be collected in GlueX during the first one to two years of running. There are several assumptions that need to be made to make these estimates.

- 1 There will be 26 weeks of 12 GeV operation with beam on the GlueX target. Of the 26 weeks, $\frac{1}{3}$ of it will produce useful data. This leads to 5×10^6 seconds of good beam per year.
1. Initially, the GlueX Detector will be able to handle a photon flux of 10^7 tagged photons per second on target. We hope that this number will quickly be increased to 10^8 tagged photons per second.
2. The combination of solid angle and reconstruction efficiency will allow us to use 72% of the events that are collected to tape.

Using a 30 cm long liquid Hydrogen target and various assumptions about cross sections, we arrive at the event rates given in Table 14.

σ μb	N_γ	Events		
		Trig. Rate	To Tape	Reconstructed
$1 \mu b$	$1 \times 10^7 \gamma/s$	$12.6 Hz$	$6.3 \times 10^7 yr^{-1}$	$4.5 \times 10^7 yr^{-1}$
$1 \mu b$	$5 \times 10^7 \gamma/s$	$63 Hz$	$3.2 \times 10^8 yr^{-1}$	$2.3 \times 10^8 yr^{-1}$
$1 \mu b$	$1 \times 10^8 \gamma/s$	$126 Hz$	$6.3 \times 10^8 yr^{-1}$	$4.5 \times 10^8 yr^{-1}$
$.1 \mu b$	$1 \times 10^7 \gamma/s$	$1.26 Hz$	$6.3 \times 10^6 yr^{-1}$	$4.5 \times 10^6 yr^{-1}$
$.1 \mu b$	$5 \times 10^7 \gamma/s$	$6.3 Hz$	$3.2 \times 10^7 yr^{-1}$	$2.3 \times 10^7 yr^{-1}$
$.1 \mu b$	$1 \times 10^8 \gamma/s$	$12.6 Hz$	$6.3 \times 10^7 yr^{-1}$	$4.5 \times 10^7 yr^{-1}$
$1 nb$	$1 \times 10^7 \gamma/s$	$0.0126 Hz$	$6.3 \times 10^4 yr^{-1}$	$4.5 \times 10^4 yr^{-1}$
$1 nb$	$5 \times 10^7 \gamma/s$	$0.063 Hz$	$3.2 \times 10^5 yr^{-1}$	$2.3 \times 10^5 yr^{-1}$
$1 nb$	$1 \times 10^8 \gamma/s$	$0.126 Hz$	$6.3 \times 10^5 yr^{-1}$	$4.5 \times 10^5 yr^{-1}$

Table 14: Expected event rates for various production cross sections in photo-production. The σ column is the cross section. For each listed cross section, there are three different photon rates given. We then compute the event rate to tape, the number of recorded events per year and the number of reconstructed events per year.

5.2 Event Distributions

In addition to the total number of events generated, we need to estimate how the data will be distributed as a function of the meson mass, m_X . In order to do this, we need to make some additional assumptions. We first assume that we have a base production cross section, σ for the channel of

interest and that the production follows an $e^{-5|t|}$ distribution. Looking at Figure 2 which is a plot of $|t|$ versus meson mass, we can extract the value of $|t|_{min}$ and $|t|_{max}$. For a given mass, we can integrate $e^{-5|t|}$ from $|t|_{min}$ to $|t|_{max}$. This integral is proportional to the number of events produced in a given mass bin. Carrying out such a procedure, for a distribution with 180 10 MeV wide mass bins from 1.0 to 2.8, we find that about 21% of the data is in the lowest bin and about 0.3% of the data is in the highest bin. This procedure will allow us to estimate how many events we would get in each mass bin of a experimental measurement.

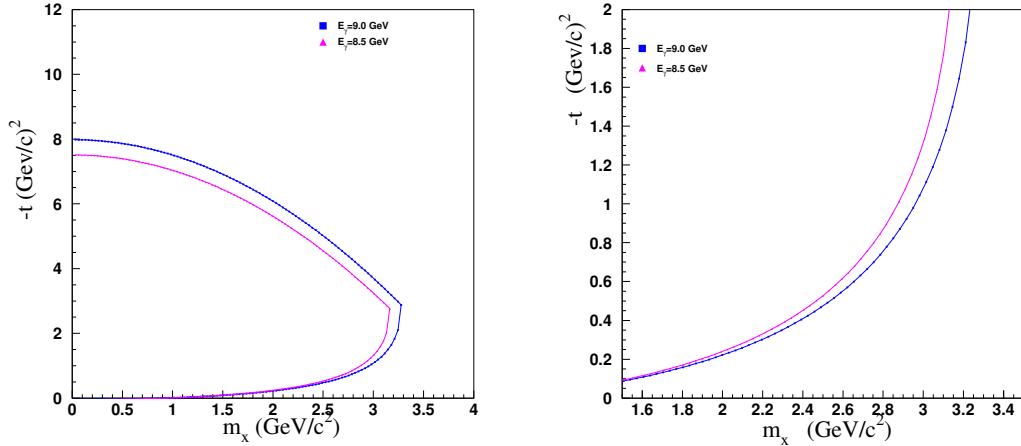


Figure 2: The limits on $|t|$ for photo-production as a function of the mass of the meson system. The left-hand plot shows the boundaries on $-t$ over all mass ranges, while the right-hand plot looks at the low- $|t|$ region for masses of interest in GlueX.

Taking a photon beam rate of $10^7 \gamma/s$ and using both a $1 \mu b$ and $10 \mu b$ total cross section in addition to the other assumptions from above, we estimate that our event spectrum will have about 4.5×10^7 and 4.5×10^8 events (respectively) after 1 year of running. These events will be distributed roughly as shown in Figure 4. As an aside, the $10 \mu b$ cross section is roughly the 3π cross section from Table 12. This data set can be compared to the current largest 3π data set in existence, that from the Brookhaven E852 experiment. A recently published result from this experiment has roughly 3×10^7 such events. In one year of running, GlueX is likely to exceed this by an order of

magnitude.

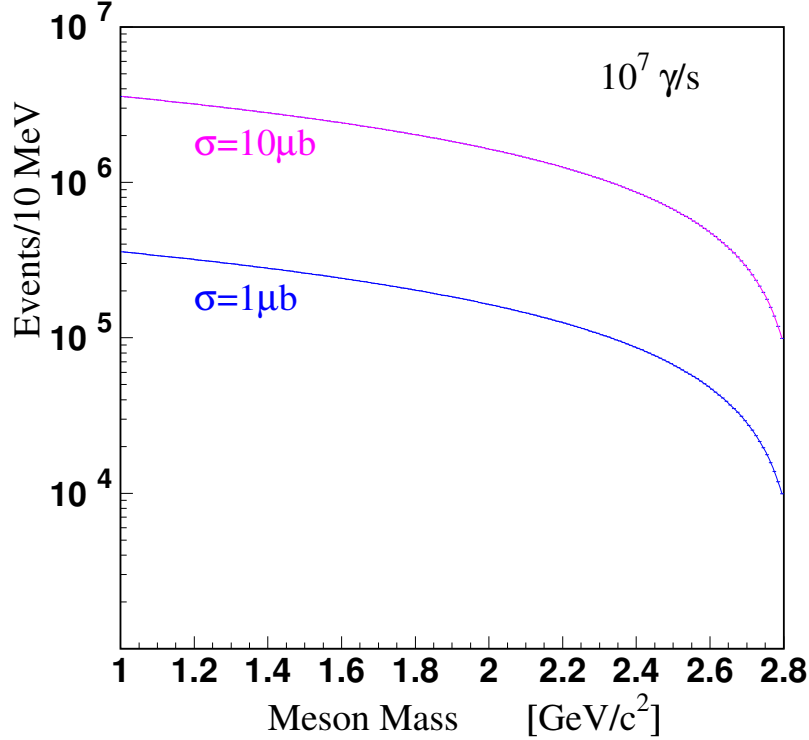


Figure 3: The estimated number of events per 10 *MeV* wide bin after one year of running With a photon flux of $10^7 \gamma/s$ for both a $1 \mu b$ and a $10 \mu b$ total cross section.

As will be seen in the following section, a potentially better way to present the data is to determine how long it takes to get a certain number of events in each mass bin in the experiment. Because it would be useful to be able to break some of the mass bins into $|t|$ bins as well, we have chosen the number of 50,000 events in each bin. At this point, this is only a reference. In the current CMU analysis of CLAS data, we have the bin width starting out at 10 *MeV* where there is data, then increasing to 20 *MeV* and eventually 40 *MeV*. To do physics in low statistics bins, these tricks will be necessary. We also find in CLAS that 10,000 events per bin is actually quite good statistics. However, given these caveats, in Figure 4 are shown how long (in

years) it would take to acquire 50,000 events in a given mass bin for the shown cross section and the assumptions that were made above.

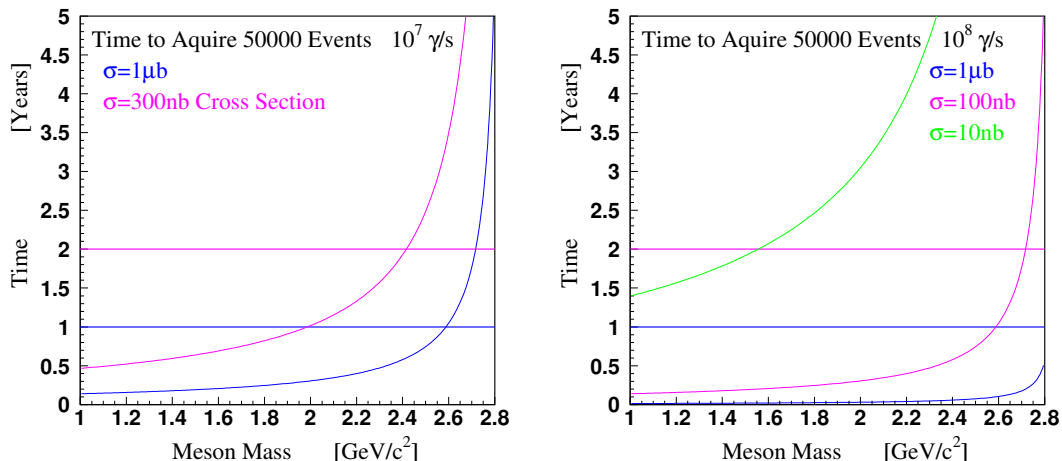


Figure 4: The time in years required to collect 50000 events in a given 10 MeV wide mass bin. The left-hand figure assumes a photon rate of $10^7 \gamma/s$, while that on the right assumes $10^8 \gamma/s$.

6 Potential Physics in The First Years

Estimating the sensitivity to final states requires a number of assumptions. The PWA is carried out in each mass bin of the data. We could increase bin-by-bin statistics by going from 10 to 20 MeV wide bins. However, if we want to know something about the t -distribution of a given bin, we will need to divide things into several t -bins. Probably a safe assumption is that we need about 50,000 counts in a given mass bin to be able to carry out a solid measurement. For a small signal, we need about 1% of this number per bin over about 10 bins, or on the order of 5000 events. This is roughly a 0.5 nb cross section at 10^7 and a 0.05 nb cross section at 10^8 . The left hand plot in Figure 4 shows how long one would need to run at 10^7 photons per second to reach the 25000 number for a $1 \mu\text{b}$ cross section. Essentially, for masses below about $2.4 \text{ GeV}/c^2$, this will be met in a year of running.

In Table 15 are presented known decays of several well established mesons. Many of these will be daughter products in the decays of interest in GlueX and all of them have been used in other partial wave analysis in the past.

Particle Name	Mass GeV/c^2	Width GeV/c^2	Decay Mode	Decay Fraction
η	0.548	1.29keV	$\gamma\gamma$	0.3943
			$\pi^0\pi^0\pi^0$	0.3251
			$\pi^+\pi^-\pi^0$	0.26
η'	0.958	0.202MeV	$\pi^+\pi^-\eta$	0.443
			$\rho^0\gamma$	0.295
			$\pi^0\pi^0\eta$	0.209
			$\gamma\gamma$	0.0212
ω	0.782	8.49MeV	$\pi^+\pi^-\pi^0$	0.891
			$\pi^0\gamma$	0.0892
ϕ	1.019	4.26MeV	K^+K^-	0.491
			K_LK_S	0.340
$b_1(1235)$	1.229	0.142	$\omega\pi$	1.00
$f_2(1270)$	1.275	0.185	$\pi^+\pi^-\pi^0$	0.154
			$\pi\pi$	0.848
$f_1(1285)$	1.282	0.024	$K\bar{K}$	0.046
			$\eta\pi\pi$	0.52
$\eta(1295)$	1.294	0.055	4π	0.331
			$K\bar{K}\pi$	0.090
			$\rho^0\gamma$	0.055
			$\eta\pi\pi$	
			$K\bar{K}\pi$	
$a_2(1320)$	1.318	0.110	$\rho\pi$	0.701
			$\eta\pi$	0.145
			$K\bar{K}$	0.049
$f_2'(1525)$	1.525	0.073	$\eta'\pi$	0.0053
			$K\bar{K}$	0.888
			$\eta\eta$	0.103
			$\pi\pi$	0.0082

Table 15: Decay channels and rates of mesons that are may be relevant to early GlueX analysis.

6.1 Calibration Reactions

6.1.1 Production of the $a_2(1320)$

If we look back to Table 12, we note the production cross section for the $a_2(1320)$ is about $1\mu b$ in the reaction

$$\gamma p \rightarrow a_2^+(1320)n.$$

This is both a large cross section, and at a mass where GlueX will very quickly be able to accumulate statistics. We also note that in Table 15, that there are several possible decay channels for the a_2 . If we put all this information together, and then carry decays through to pions, kaons and photons, we find arrive at the following information.

$$\begin{aligned} a_2^+(1320) \rightarrow \quad \rho\pi &\rightarrow \quad \pi^+\pi^+\pi^- \\ &\quad \pi^+\pi^0\pi^0 \\ \pi^+\eta &\rightarrow \quad \pi^+\gamma\gamma \\ &\quad \pi^+\pi^+\pi^-\pi^0 \\ &\quad \pi^+\pi^0\pi^0\pi^0 \\ K^+K_S &\rightarrow \quad K^+\pi^+\pi^- \\ &\quad K^+\pi^0\pi^0 \\ \pi^+\eta' &\rightarrow \quad \pi^+\pi^+\pi^-\gamma\gamma \end{aligned}$$

These final states taken as a whole do a very good job in mapping out the response of the entire GlueX detector. There are all charged final states, mostly neutral final states, and final states with kaons, and secondary vertices from the K_S decays. In addition, if one can believe the various branching fractions, then all of these final states should give the same production cross section and differential production cross sections for the a_2 meson. Getting all of these to agree will be an excellent way to make sure that we fully understand the GlueX detector and its efficiencies.

From this, we should carry out *a detailed mapping of the a_2 production and differential cross sections using many different final states*. This study will allow us to study and understand all aspects of the GlueX detector.

6.1.2 Vector Meson Production and Polarization Transfer

The three lightest vector mesons, the ρ , ω and ϕ are all produced with relatively large cross sections in GlueX. Given that they are all spin-one

particles, they can carry polarization which can be measured by looking at their decays into pseudo-scalar mesons. *A detailed measurement of both the production and polarization of these particles* would be a useful program which would involve the linear polarization of the beam in a reasonable way.

6.1.3 Higher Mass Vector Mesons

Photo production is the natural reaction in which to produce vector mesons. The higher mass vector mesons are also in a fairly confused state. The Particle Data Book [18] lists the states in Table 16. Pulling these states out of the background will require a detailed partial wave analysis, but it is expected that the signals would be large, perhaps dominating some of the final state channels. In addition, the information on these states is fairly confused and new information would help settle a number of issues. There is also at least one ϕ state missing. While an initial study of these states is

Particle Name	Mass GeV/c^2	Width GeV/c^2	Decays
$\rho(1450)$	1.465	0.400	$\pi\pi, 4\pi, \omega\pi$
$\rho(1700)$	1.720	0.250	$\pi\pi, 4\pi$
$\omega(1420)$	1.400	0.250	$\rho\pi, \omega\pi\pi$
$\omega(1650)$	1.670	0.315	$\rho\pi, \omega\pi\pi$
$\phi(1680)$	1.680	0.150	$K\bar{K}^* + cc, K\bar{K}$

Table 16: A list of known vector mesons with their masses and main decay modes.

not likely to settle things, there is a 1^{--} nonet of hybrids that could overlap with the expected quark-antiquark states. There are model predictions on expected decay rates for all of these states, but to date the data have not been good enough to resolve things.

6.2 Hybrid Meson Searches

The search for exotic hybrids is the *mantra* of GlueX, and any physics program needs to include this as a significant component. This is especially true of the initial running of GlueX. Looking over all the information tabulated in this report, we have identified three final states that are likely to be good candidates for exotic hybrid searches in the early years of GlueX. These are

3π , $\eta\pi\pi$ and $\omega\pi\pi$. In Table 17 we show these channels with their estimated cross sections with the likely decay of of the η or ω that would be used. Using this information, we have predicted the number of each such event that would be collected in GlueX. These are shown in Figure 5, although we need to point out that some additional assumptions were made. The 3π sample is collected in 3 months and the data shown are in 10 MeV wide bins. Both the $\eta\pi\pi$ and $\omega\pi\pi$ are binned in 20 MeV wide bins. The ω sample is collected in 1 year of running, while the η sample would take the full two years. For masses up to about $2\text{ GeV}/c^2$, we would have at least 50000 events per bin, while we would have at least 20000 events per bin up to masses of about $2.5\text{ GeV}/c^2$.

Reaction	σ	Fin St.	BR
$\gamma p \rightarrow p\pi\pi\pi$	$10\mu b$	3π	1.0
$\gamma p \rightarrow n\pi^+\pi\pi$	$10\mu b$	3π	1.0
$\gamma p \rightarrow p\pi\pi\omega$	$0.2\mu b$	3π	0.88
$\gamma p \rightarrow n\pi^+\pi\omega$	$0.2\mu b$	3π	0.88
$\gamma p \rightarrow p\pi\pi\eta$	$0.2\mu b$	$\gamma\gamma$	0.37
$\gamma p \rightarrow n\pi^+\pi\eta$	$0.2\mu b$	$\gamma\gamma$	0.37

Table 17:

Given these three event samples, it would be possible to carry out searches for the several exotic hybrid mesons. In the 3π channel, searches would be made for hybrids that couple to either $\rho\pi$ or $f_2(1270)\pi$. This includes the π_1 and the h_2 . In the $\omega\pi\pi$ final state, we would search for hybrids decaying to $b_1(1235)\pi$ and $f_2(1270)\omega$. This includes the h_0 , π_1 and the h_2 . Finally, the $\eta\pi\pi$ final state allows us to search for exotic hybrids that decay to $a_2\pi$, $\eta\rho$ and $\eta f_2(1270)$. This includes the η_1 and the b_2 . The results are summarized in Table 18, but the important point is that in principle we have access to hybrids from each of the three exotic nonets. Also, for most of these, there are more than one decay mode that could be measured.

7 Conclusions

The GlueX experiment can expect a very solid physics program from its first two years of running, even under very modest assumption of only $10^7\gamma/s$. This program will allows us to understand the detector, polarization and

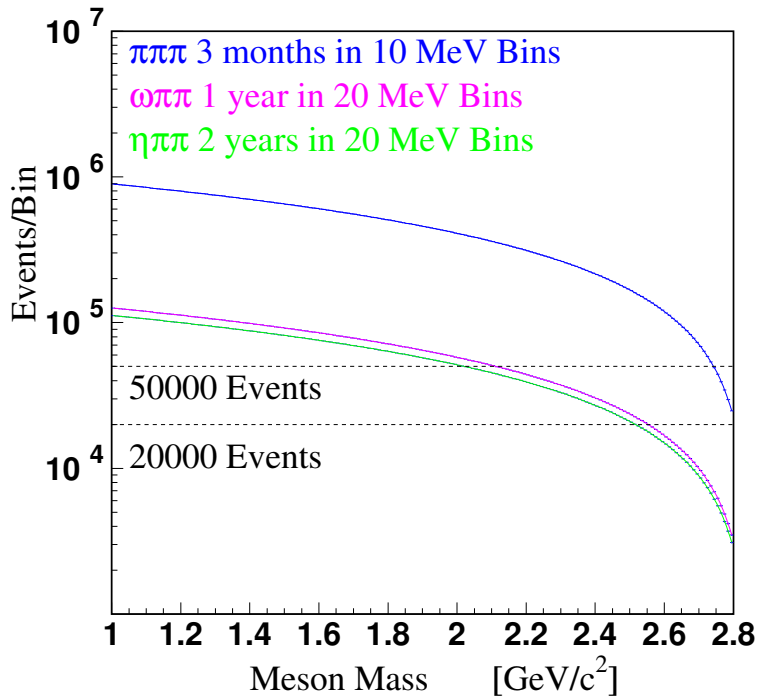


Figure 5: Rates for the three final states listed in Table 17. All data assume $10^7 \gamma/s$ on target.

Hybrid	$\pi\pi\pi$	$\omega\pi\pi$	$\eta\pi\pi$
h_0	yes	yes	
η_1			yes
π_1	yes	yes	
h_2		yes	
b_2	yes		yes

Table 18: A summary of which exotic hybrids can be observed in which of the three final states.

systematics by studying the $a_2(1320)$ and the light vector mesons, ρ , ω and ϕ . There will be an interesting program studying the properties of the excited vector mesons. And finally, we will have the potential to access exotic hybrids in all three exotic nonets, and to look for multiple decay modes for several

of these. Such a program could well establish the hybrid spectrum and start to shed real lights on its properties.

However, to be fully understand things, and in particular to be able to do channels with K 's in the final state, rates are going to need to increase to at least 5×10^7 and higher if possible. This will allow us to collect sufficient statistics in a two year period for a significant more comprehensive search. Even rarer channels are going to require running for longer periods of time at higher rates.

References

- [1] **The GlueX Design Report, Version 4**
- [2] C. A. Meyer, **A summary of expected event rates in GlueX**, GlueX-doc **438**, February 2005.
- [3] C. A. Meyer **A Summary of Hybrid Masses and Decays**, GlueX-doc **380**, November 2004.
- [4] P. Lacock *et al.*, Phys. Lett. B**401**, 309, (1997), hep-lat/9611011.
- [5] C. Bernard *et al.*, Phys. Rev. D**56**, 7039, (1997).
- [6] C. Bernard *et al.*, **Exotic meson spectroscopy from the clover action at $\beta = 5.85$ and 6.15**, Nucl. Phys. B(Proc. Suppl.) **73**, 264, (1999), hep-lat/9809087.
- [7] P. Lacock, K. Schilling (SESAM Collaboration), **Hybrid and Orbitally Excited Mesons in Full QCD**, Nucl. Phys. Proc. Suppl. **73**, 261, (1999), hep-lat/9809022.
- [8] Zhong-Hao Mei and Xiang-Qian Luo, **Exotic mesons from quantum chromodynamics with improved gluon and quark actions on the anisotropic lattice**, Nucl. Phys. Proc. Suppl. **119**, 263, (2003), (hep-lat/0206012).
- [9] C. Bernard, T. Burch, C. DeTar, Steven Gottlieb, E.B. Gregory, U.M. Heller, J. Osborn, R. Sugar and D. Toussaint, Phys. Rev. D**68**, 074505, (2003).
- [10] C. Morningstar, **The study of exotic hadrons in lattice QCD**.
- [11] P. R. Page, E. S. Swanson and A. P. Szczepaniak, **Hybrid Meson Decay Phenomenology**, Phys. Rev. D**59**, 034016 (1999).
- [12] N. Isgur, R. Kokoski and J. Paton, **Gluonic Excitations of Mesons: Why they are missing and where to find them**, Phys Rev Lett. **54**, 869, (1985).

- [13] H.P. Shanahan, *et al.* (UKQCD Collaboration), **The effect of tree-level and mean-field improvement on the light-hadron spectrum in quenched QCD**, Phys. Rev. D**55**, 1548, (1997), hep-lat/9608063.
- [14] P. Lacock, C. Michael, P. Boyle, P. Rowland (UKQCD Collaboration), **Orbitally excited and hybrid mesons from the lattice**, Phys. Rev. D**54**, 6997, (1996), hep-lat/9605025. K
- [15] P. Lacock, C. Michael, P. Boyle and P. Rowland (UKQCD Collaboration), **Hybrid and Orbitally Excited Mesons in Quenched QCD**, Nucl. Phys. Proc. Suppl. **63**, 203, (1998), hep-lat//9708013.
- [16] K. J. Juge, J. Kuti and C. Morningstar, Phys. Rev. Lett. **82**, 4400, (1999).
- [17] T. Manke *et al.*, Phys. Rev. Lett. **82**, 4396, (1999).
- [18] S. Eidelman, *et al.*, **Review of Particle Properties**, Phys. Lett. B**592**, 1, (2004).